

A Phenomenological Approach to Heavy Majorana Mass Neutrinos in Dileptonic and Trileptonic Channels at Hadron Colliders

Emrah Tıraş^{ID}*1,2, Kamuran Dilsiz^{ID}3, Ayşe Bat^{ID}1

¹Department of Physics, Faculty of Science, Erciyes University, Kayseri 38280, Türkiye

²Department of Physics and Astronomy, University of Iowa, IA 52242, USA

³Department of Physics, Faculty of Art and Science, Bingöl University, Bingöl 12000, Türkiye

(Alınış / Received: 16.05.2022, Kabul / Accepted: 08.08.2022, Online Yayınlanma / Published Online: 23.08.2022)

Keywords

Neutrinos,
Heavy Majorana Neutrinos,
Large Hadron Collider (LHC),
Alpgen,
HVYN package,
LHC experiment.

Abstract: The non-zero masses of neutrinos are the first solid evidence beyond the Standard Model of particle physics. Seesaw mechanism is one of the extensions to the Standard Model, which is generating Majorana type light neutrinos with corresponding heavy neutrino mass states. In this model, the smallness of the light neutrino mass ($\nu_\mu < 1$ eV) is explained by having heavy neutrino mass at the TeV scale that is an accessible regime at particle colliders. In this paper, we describe a phenomenological study on heavy Majorana neutrino productions in proton-proton collisions at center-of-mass energies of 8 and 13 TeV. We consider that the heavy Majorana neutrino is produced by both dileptonic and trileptonic channels as production of a charged W boson. The cross section results of the heavy Majorana neutrinos for both same-sign and opposite-sign events in the dileptonic channel show a similar trend for the higher mass region starting from 300 GeV/c² when a $p_T > 5$ GeV/c cut applied on leptons. The results also show that the production of such heavy mass neutrino particles is more likely to happen in the dileptonic channel than in the trileptonic channel.

Hadron Çarpıştırıcılarında İki-leptonik ve Üç-leptonik Kanallarda Ağır Majorana Nötrino Araştırmalarına Fenomenolojik Yaklaşım

Anahtar Kelimeler

Nötrinolar,
Ağır Majorana Nötrinoları,
Büyük Hadron Çarpıştırıcısı
(BHÇ),
Alpgen,
HVYN paketi,
BHÇ deneyleri

Özet: Nötrinoların kütlelerinin sıfırdan farklı olması, parçacık fiziğindeki Standart Modelin ötesindeki ilk somut kanıttır. Seesaw mekanizması, ağır nötrino kütle durumlarına karşılık gelen Majorana tipi hafif nötrinolar üreten Standart Modelin uzantılarından biridir. Bu modelde, hafif nötrino kütlelerinin ($\nu_\mu < 1$ eV) küçüklüğü, parçacık çarpıştırıcıları ile erişilebilir olan TeV ölçeğindeki ağır nötrino kütlesi ile açıklanmaktadır. Bu makalede, kütle merkezi enerjileri 8 ve 13 TeV olan proton-proton çarpışmalarındaki ağır Majorana nötrino üretimleri üzerine fenomenolojik bir çalışma sunulmaktadır. Ağır Majorana nötrinolarının yüklü W bosonlarının aracılığı ile üretilen hem iki-leptonik hem de üç-leptonik üretim kanalları dikkate

alınmıştır. İki-leptonik kanaldaki hem aynı işaretli hem de zıt işaretli olaylar için ağır Majorana nötrinolarının tesir kesiti sonuçları leptonlar üzerine $p_T > 5 \text{ GeV}/c$ limiti uygulandığında $300 \text{ GeV}/c^2$ 'den başlayarak daha yüksek kütleli bölgeler için benzer bir eğilim göstermektedir. Ayrıca sonuçlar bu tür ağır kütleli nötrino parçacıklarının üretiminin ikileptonik kanalda trileptonik kanala göre daha olası olduğunu göstermektedir.

*Corresponding Author, email: etiras@fnal.gov

1. Introduction

The CMS [1] and ATLAS [2][3] experiments, state-of-art particle detectors have been collecting data since the Large Hadron Collider (LHC) started to smash high energetic proton bunches in 2007. The center-of-mass energy at the LHC was 7 TeV in 2011, 8 TeV in 2012, and it reached 13 TeV in 2015. The design collision energy of the LHC is 14 TeV, and it is aimed to reach to that in the near future.

The LHC has been the source of many exotic particles since it started to run. As weakly interacting particles, Neutrinos are not interacting with the detectors much, but the interaction of daughter particles (from the neutrino interactions) with the active detector elements nuclei can be reconstructed to understand neutrino nature. The discovery of the neutrino oscillations established that neutrinos cannot be zero-mass particles as predicted by the Standard Model (SM) [4-6]. The tiny mass values of the observed neutrinos are explained with various extension models to the SM. Among those, Seesaw model type-I [7-15] is one of the most common mechanisms, which is generating light neutrinos with a corresponding heavy neutrino mass state, N . Both light and heavy neutrinos are Majorana type particles, and the lepton number conservation is violated by two units in the Majorana nature of neutrinos. In this model, the light neutrino mass is inversely related to the heavy mass neutrino state, so the smallness of the light neutrino (m_ν) is explained by the largeness of the heavy mass state N (M_N), $m_\nu \approx y_\nu^2 v^2 / M_N$, where y_ν is a Yukawa coupling and v is the Higgs vacuum expectation value in the SM. The numerator in the equation gives the Dirac type neutrino mass, $m_D^2 = y_\nu^2 v^2$. The existence of heavy mass neutrino may help us to reveal the nature of neutrino masses and may also be a possible candidate for dark matter, which can help us explain the matter-antimatter asymmetry problem [16-22].

$$V_{lN} = \begin{bmatrix} V_{eN_1} & V_{eN_2} & V_{eN_3} \\ V_{\mu N_1} & V_{\mu N_2} & V_{\mu N_3} \\ V_{\tau N_1} & V_{\tau N_2} & V_{\tau N_3} \end{bmatrix} \quad (1)$$

Majorana studies have long been studied in accelerator-based hadron colliders like at Large Electron-Positron (LEP) Collider and the LHC some limits were set on the mixing matrix, V_{lN} in Eq. 1 shows the different flavor combinations and mixing parameters between heavy mass state and lepton flavors, as shown in the Feynman diagrams, Fig. 1.

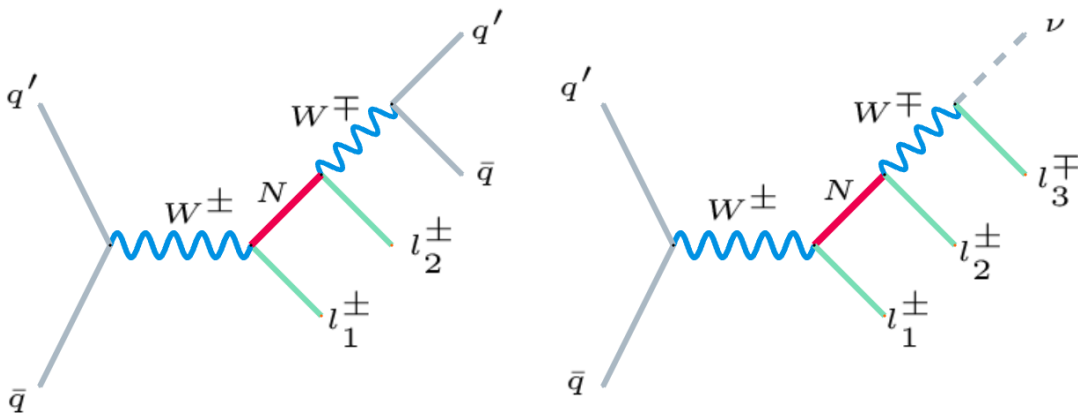


Figure 1. The Feynman diagrams of dileptonic (left) and trileptonic (right) resonant production of heavy Majorana neutrino in proton-proton collisions.

Previously, the L3 [23] and DELPHI [24] experiments at LEP searched the Majorana neutrinos for $Z \rightarrow \nu_l N$ ($l = e, \mu, \tau$) decay channel and put limits on $|V_{\nu N}|^2$ as a function of m_N . Table 1 shows the limits on $|V_{\mu N}|^2$, $|V_{eN}|^2$, and $|V_{eN} V_{\mu N}^*|^2 / |V_{eN}|^2 + |V_{\mu N}|^2$ arising from different dileptonic channels ($\mu^\pm \mu^\pm, e^\pm e^\pm, e^\pm \mu^\pm / \mu^\pm e^\pm$) for the corresponding run-periods by the CMS experiment at CERN. The ATLAS experiment also reported the results for heavy Majorana neutrinos at the center of mass energies of 8 TeV [25] and 13 TeV [26].

Table 1. CMS detector heavy Majorana search results for Dileptonic final state using 7 TeV (5.0 fb⁻¹) [27], 8 TeV (19.7 fb⁻¹) [28][29], and 13 TeV (35.9 fb⁻¹) [30].

	7 TeV (5.0 fb ⁻¹)	8 TeV (19.7 fb ⁻¹)	13 TeV (35.9 fb ⁻¹)
$ V_{\mu N} ^2$	$7.0 \times 10^{-2} M_N = 90 \text{ GeV}$ $4.3 \times 10^{-1} M_N = 203 \text{ GeV}$	$4.7 \times 10^{-3} M_N = 90 \text{ GeV}$ $1.23 \times 10^{-2} M_N = 200 \text{ GeV}$ $5.83 \times 10^{-1} M_N = 500 \text{ GeV}$	$2.31 (1.9) \times 10^{-5} M_N = 40 \text{ GeV}$ $2.7 (1.6) \times 10^{-1} M_N = 1000 \text{ GeV}$
$ V_{eN} ^2$	$2.2 \times 10^{-1} M_N = 90 \text{ GeV}$ $4.3 \times 10^{-1} M_N = 203 \text{ GeV}$	$2.0 \times 10^{-2} M_N = 90 \text{ GeV}$ $1.7 \times 10^{-2} M_N = 200 \text{ GeV}$ $7.1 \times 10^{-1} M_N = 500 \text{ GeV}$	$9.5 (8.0) \times 10^{-5} M_N = 40 \text{ GeV}$ $4.2 (3.2) \times 10^{-1} M_N = 1000 \text{ GeV}$
$\frac{ V_{eN} V_{\mu N}^* ^2}{ V_{eN} ^2 + V_{\mu N} ^2}$	Not Available	$5.0 \times 10^{-3} M_N = 90 \text{ GeV}$ $5.0 \times 10^{-3} M_N = 200 \text{ GeV}$ $2.9 \times 10^{-1} M_N = 500 \text{ GeV}$	$2.7 (2.7) \times 10^{-5} M_N = 40 \text{ GeV}$ $1.4 (1.4) \times 10^{-1} M_N = 1000 \text{ GeV}$

In this study, we have simulated heavy Majorana neutrino production and decay processes in both dileptonic (also known as s-channel, see Figure 1-left) and trileptonic (also known as t-channel, see Figure 1-right) using a custom, leading order (LO) Alpgen event generator (v2.14) [31] with LO parton distribution functions (PDFs), CTEQ6L and CTEQ6L1, and with next-to-leading order (NLO) PDF, CTEQ6M [32][33]. The interactions of Majorana neutrinos (N) with the charged lepton (l^\pm) and charged boson (W^\pm) as a mediated process are show in Equation 2, and the corresponding Feynman diagrams are shown in Figure 1.

$$\begin{aligned}
pp &\rightarrow l_1^\pm N, \quad N \rightarrow l_2^\pm W^\mp, \quad W^\mp \rightarrow jj && \text{(dileptonic)} \\
pp &\rightarrow l_1^\pm N, \quad N \rightarrow l_2^\pm W^\mp, \quad W^\mp \rightarrow l_3^\pm \nu && \text{(trileptonic)}
\end{aligned} \tag{2}$$

2. Methods and Simulation

2.1. Simulation of s-channel and t-channel heavy neutrino mass production

For physics processes of heavy Majorana neutrino production in hadron-hadron collisions, the HVYN package in the ALPGEN v2.14 framework was developed and implemented by F. del Aguila et al. [34]. The code was written in Fortran, a common compiled imperative programming language in 1950s, and we have written a bash script to enable robust computation.

The SM provides LO matrix element calculations of $d\hat{\sigma}$ based on the ALPHA algorithm with common LO (CTEQ6L, CTEQ6L1, etc.) and NLO (CTEQ6M, etc.) PDF sets. In the HVYN package, both weighted and unweighted parton level event generations are possible. Weighted event generation is sufficient to produce results at the parton level, but in this study, we generated unweighted events to produce actual events, which can provide more realistic detector simulation studies for the particle interactions. During the unweighting stage, kinematics, flavors, colors, and spins of the events are reconstructed. Therefore, the cross sections in this study were calculated based on unweighted events with all the kinematics of the particles. Also, the particle selection process was done during the parton level to select only required particles in the final state.

At 8 TeV proton-proton (pp) collision energy, 50k unweighted events were generated at each mass point of the heavy Majorana mass state were generated. However, to have more statistics at 13 TeV pp collision energy, we generated 200k events for each selected mass point of the heavy Majorana mass state in the low mass region, 40-90 MeV, 100k events in the intermediate mass region, 100-300 MeV and 50k events in the high mass region, 350-1500 MeV. Event samples at each mass point were generated for both dilepton ($ee, \mu\mu, \mu e, e\mu$) and trilepton ($eee, e\mu\mu, e\mu e, e\mu\mu, \mu\mu e, \mu\mu\mu$) final state of the heavy Majorana mass neutrino production.

In this search channel of the heavy Majorana neutrinos at pp collisions, the study is pursued in dileptonic and trileptonic final-state combinations of electrons (e) and muons (μ) except taus (τ) since the mean lifetime of tau is so short, and it's challenging to reconstruct taus in accelerator experiments. For comparison purposes, the same-sign (SS) and opposite-sign (OS) final state dilepton and trilepton events were generated. For further analysis with more statistics, the outputs of the SS and OS events as in Les Houches Event (LHE) files at each mass point were carefully combined by using a Python script.

In the pp collisions, there are three potential sources for SS dilepton event candidates; the first one is WZ production, in which two prompt SS leptons are identified, and the other two are $Z \rightarrow l^+l^-$ and $W^\pm W^\mp \rightarrow l^+\nu l^-\nu$, in which the charge of one of the lepton pairs is mismeasured. The latter source is an important background for dielectron studies, but it is negligible for other lepton pairs such as dimuon and electron-muon studies.

In this study, we calculated the estimates for heavy Majorana neutrino production at pp collisions for the two regimes: $m(N) < M_w$ and $m(N) > M_w$. The former case is an off-shell production in which W is a virtual particle, and reconstruction of the heavy Majorana mass and surpassing the background wouldn't be easy. On the other hand, the latter case is an on-shell production that reduces the background further and allows to be reconstructing the mass of heavy state.

3. Results

Figure 2 compares LO cross section predictions at 8 and 13 TeV of pp collisions as a function of the heavy Majorana neutrino mass (N). The selected mass points are the mass points used officially for 8 TeV and 13 TeV physics analyses by CMS Collaboration at CERN. The cross section prediction is at least a factor of 2 higher at 13 TeV than at 8 TeV in all mass regions except at 90 GeV/c².

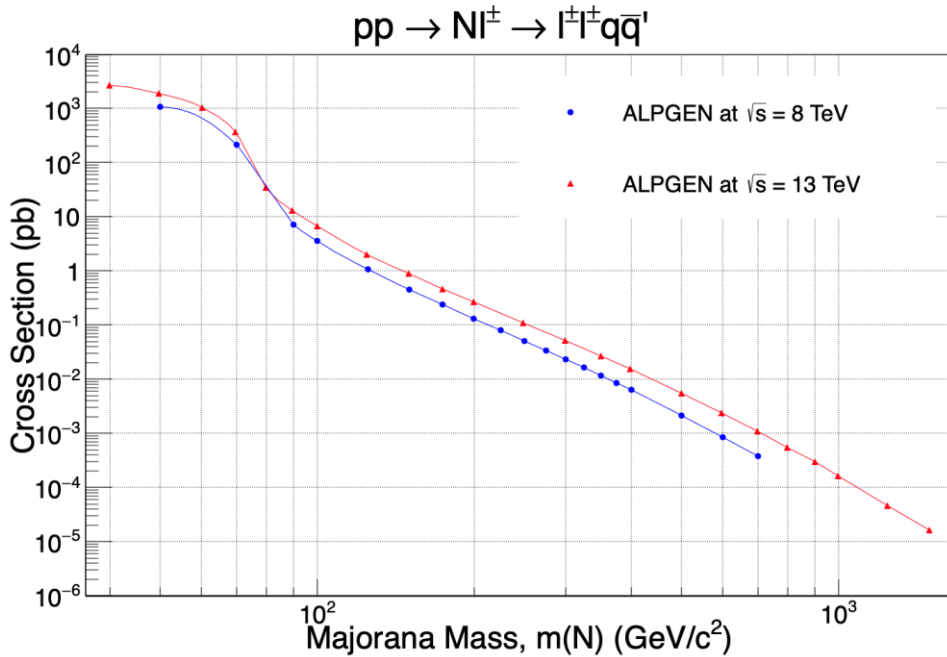


Figure 2. Leading order cross section for resonance production of a Majorana neutrino as a function of Majorana neutrino mass, N.

3.1 Dileptonic Final State

Majorana neutrino production channel, which has two leptons at the final state produced via s-channel with a different processes is shown in Equation 3. Depending on the sign of the W boson, the first lepton could be l^- or l^+ and N, the heavy Majorana, could decay l^+W^- or l^-W^+ leading to the final events containing two leptons with same-sign (SS) or opposite-sign (OS).

$$pp \rightarrow l_1^+ N, \quad N \rightarrow l_2^+ W^-, \quad W^- \rightarrow jj, \quad l = e, \mu \text{ (SS)}$$

$$pp \rightarrow l_1^- N, \quad N \rightarrow l_2^- W^+, \quad W^+ \rightarrow jj, \quad l = e, \mu \text{ (SS)}$$

$$\begin{aligned}
pp &\rightarrow l_1^+ N, \quad N \rightarrow l_2^- W^+, \quad W^+ \rightarrow jj, \quad l = e, \mu \text{ (OS)} \\
pp &\rightarrow l_1^- N, \quad N \rightarrow l_2^+ W^-, \quad W^- \rightarrow jj, \quad l = e, \mu \text{ (OS)}
\end{aligned} \tag{3}$$

The heavy Majorana neutrino production and decay processes, Figure 3, are simulated using the LO event generator described in [34] and implemented in ALPGEN v2.14 with the NLO CTEQ6M PDF at the center-of-mass energy, $\sqrt{s} = 13$ TeV as a function of Majorana neutrino mass. Figure 3 shows the cross section of heavy Majorana mass neutrinos for both SS and OS dilepton ($\mu\mu$ in this case) events. In the left plot, there is no transverse momentum (p_T) cut on leptons, and this plot shows a discrepancy at the higher Majorana mass. In the right plot, a selection cut of $p_T > 5$ GeV/c is applied to the leptons, and the plot shows that SS and OS cross section results are compatible with the optimized P_T cut on leptons.

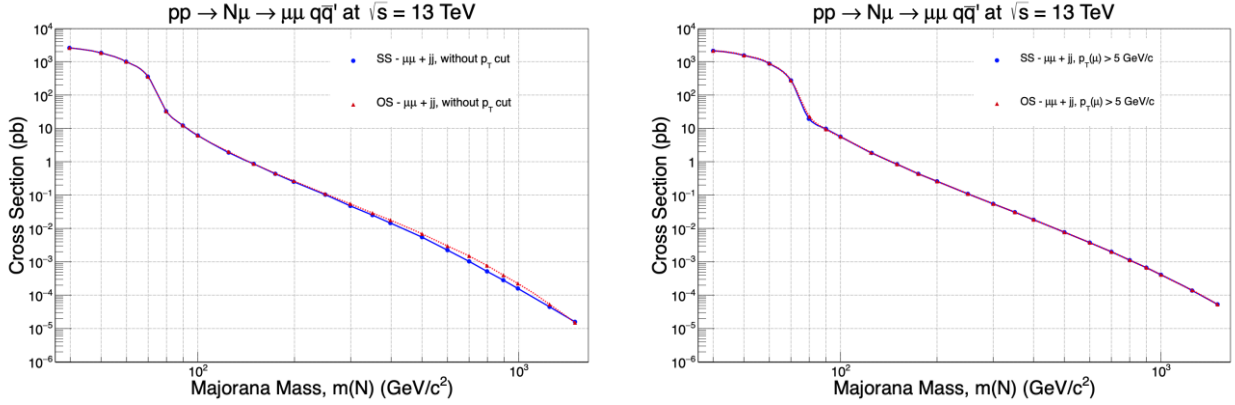


Figure 3. Cross section of Majorana neutrinos at $\sqrt{s} = 13$ TeV as a function of the mass of Majorana particles, N . The left-plot shows the cross section results of same-sign and opposite-sign final state lepton pairs without a p_T cut on the leptons, and the right-plot is with a $p_T > 5 \sim \text{GeV}/c$ cut on leptons.

Figure 4 shows the cross section results that are calculated using LO event generator with the CTEQ6M PDFs at $\sqrt{s} = 13$ TeV. The left plot shows the comparison of dilepton channels $\mu\mu$, ee , $e\mu/\mu e$, and the right plot shows the comparison of the different PDFs; CTEQ6M (NLO), CTEQ6L (LO) and CTEQ6L1 (LO) for the $\mu\mu$ final state. On the left plot, the results for $\mu\mu$ and ee dileptonic channels are similar, but they have slightly higher cross section values compared to the $e\mu/\mu e$ dileptonic channel at the higher mass region starting from 300 GeV/c². The different PDFs with LO and NLO show the indistinguishable results for dileptonic channels.

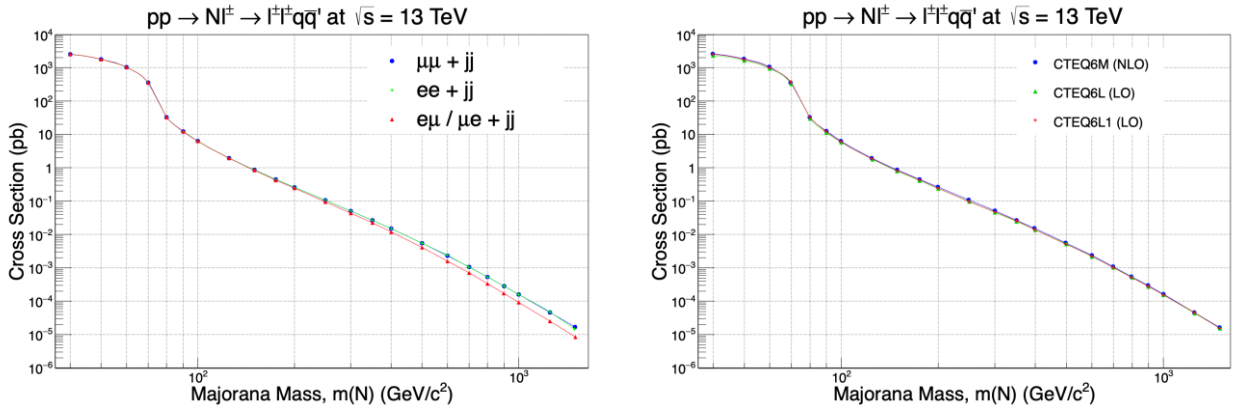


Figure 4. Cross section of Majorana neutrinos at $\sqrt{s} = 13$ TeV as a function of the mass of Majorana particles, N . The left plot shows the results for dilepton channels ($\mu\mu$, ee , $e\mu/\mu e$), and the right plot is the comparison of the different PDFs (CTEQ6M, CTEQ6L, CTEQ6L1) for the $\mu\mu$ final state.

3.2 Trileptonic Final State

$$\begin{aligned}
pp &\rightarrow l_1^+ N, \quad N \rightarrow l_2^+ W^-, \quad W^- \rightarrow l_3^- \nu, \quad l = e, \mu \text{ (SS)} \\
pp &\rightarrow l_1^- N, \quad N \rightarrow l_2^- W^+, \quad W^+ \rightarrow l_3^+ \nu, \quad l = e, \mu \text{ (SS)}
\end{aligned}$$

$$\begin{aligned}
pp &\rightarrow l_1^+ N, \quad N \rightarrow l_2^- W^+, \quad W^+ \rightarrow l_3^+ \nu, \quad l = e, \mu \quad (OS) \\
pp &\rightarrow l_1^- N, \quad N \rightarrow l_2^+ W^-, \quad W^- \rightarrow l_3^- \nu, \quad l = e, \mu \quad (OS)
\end{aligned} \tag{4}$$

The trileptonic final state processes and possible interactions are listed below in Equation 4. The 3rd lepton in the trileptonic final state comes from the W boson decaying into a lepton and a neutrino in the final state instead of two jets. Like the case in the dileptonic final state, the state of being SS or OS depends on the lepton that forms N and on the state where N decays.

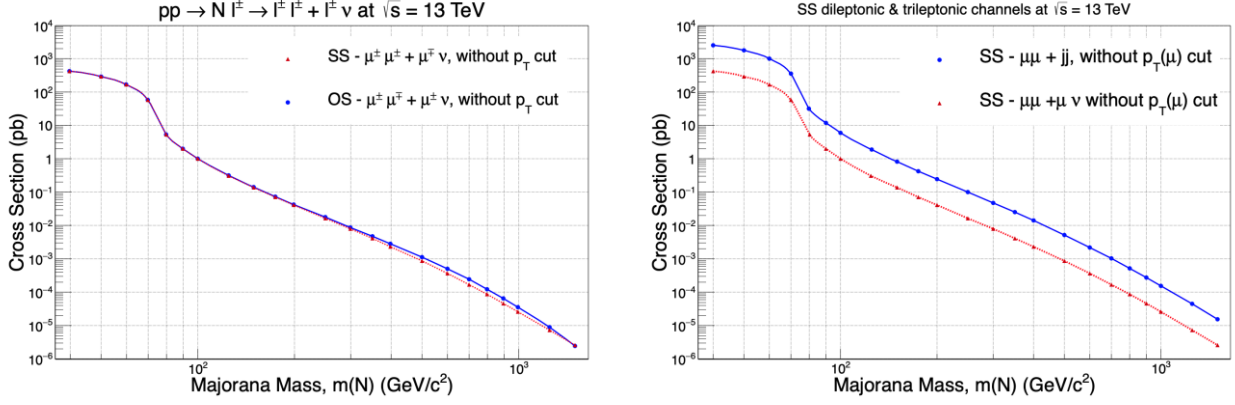


Figure 5. Cross section of Majorana neutrinos at $\sqrt{s} = 13$ TeV as a function of the mass of Majorana particles, N . The left plot shows the cross section results for same-sign and opposite-sign for trileptonic final state, and the right plot is the comparison of the dileptonic and trileptonic final state.

For the trileptonic final state, the cross section of all possible lepton flavors (eee , $\mu\mu\mu$, $e\mu\mu/e\mu e$, $e\mu\mu/\mu\mu e$) interactions are calculated by using ALPGEN v2.14 generator as described previously. Figure 5 on the left shows the SS and OS results for $\mu\mu\mu$ trileptonic final state at $\sqrt{s} = 13$ TeV without any P_T cut, and the right plot shows the comparison of the dileptonic channel for $\mu\mu + 2$ jets and the trileptonic channel produced via $\mu\mu + \mu\nu$. The cross section prediction of the dileptonic channel is almost a factor of 10 higher than the corresponding results of the trileptonic channel. This shows that dileptonic channels for heavy Majorana search at hadron colliders are more favorable than the trileptonic channels

Table 2. Cross section of Majorana neutrinos at $\sqrt{s} = 13$ TeV as a function of heavy Majorana mass, N . The table shows the comparison of the different PDFs (CTEQ6M, CTEQ6L, CTEQ6L1) for the $\mu\mu$ final state.

Mass	CTEQ6M	CTEQ6L	CTEQ6L1
40	2.654e+03	2.365e+03	2.542e+03
50	1.876e+03	1.673e+03	1.797e+03
60	1.068e+03	9.491e+02	1.023e+03
70	3.614e+02	3.327e+02	3.774e+02
80	3.331e+01	3.021e+01	3.331e+01
90	1.284e+01	1.144e+01	1.284e+01
100	6.415e+00	5.803e+00	6.143e+00
125	1.990e+00	1.804e+00	1.906e+00
150	8.735e-01	8.010e-01	8.364e-01
175	4.559e-01	4.110e-01	4.366e-01
200	2.710e-01	2.380e-01	2.485e-01
250	1.091e-01	9.721e-02	1.000e-01
300	5.219e-02	4.666e-02	4.786e-02
350	2.724e-02	2.474e-02	2.609e-02
400	1.551e-02	1.406e-02	1.422e-02
500	5.722e-03	5.222e-03	5.247e-03
600	2.404e-03	2.213e-03	2.302e-03
700	1.102e-03	1.034e-03	1.055e-03
800	5.508e-04	5.212e-04	5.274e-04
900	3.002e-04	2.786e-04	2.875e-04
1000	1.636e-04	1.569e-04	1.567e-04
1250	4.655e-05	4.463e-05	4.655e-05

1500	1.645e-05	1.550e-05	1.575e-05
------	-----------	-----------	-----------

Table 3. Cross section of Majorana neutrinos at $\sqrt{s} = 13$ TeV as a function of heavy Majorana mass, N . The table shows the cross section results for dilepton channels ($\mu\mu, ee, e\mu/\mu e$).

Mass	$\mu\mu + jj$	$ee + jj$	$e\mu/\mu e + jj$
40	2.567e+03	2.568e+03	2.569e+03
50	1.818e+03	1.817e+03	1.818e+03
60	1.031e+03	1.031e+03	1.031e+03
70	3.614e+02	3.609e+02	3.608e+02
80	3.297e+01	3.296e+01	3.300e+01
90	1.254e+01	1.253e+01	1.253e+01
100	6.374e+00	6.374e+00	6.339e+00
125	1.987e+00	1.986e+00	1.951e+00
150	8.714e-01	8.713e-01	8.450e-01
175	4.533e-01	4.530e-01	4.329e-01
200	2.623e-01	2.621e-01	2.466e-01
250	1.068e-01	1.067e-01	9.683e-02
300	5.101e-02	5.100e-02	4.446e-02
350	2.691e-02	2.691e-02	2.250e-02
400	1.520e-02	1.519e-02	1.219e-02
500	5.577e-03	5.576e-03	4.153e-03
600	2.339e-03	2.448e-03	1.631e-03
700	1.083e-03	1.085e-03	7.135e-04
800	5.432e-04	5.426e-04	3.396e-04
900	2.891e-04	2.891e-04	1.759e-04
1000	1.627e-04	1.627e-04	9.376e-05
1250	4.633e-05	4.830e-05	2.512e-05
1500	1.685e-05	1.460e-05	8.460e-06

Table 4. Cross section of Majorana neutrinos at $\sqrt{s} = 13$ TeV as a function of heavy Majorana mass, N . The table shows the cross section results of same-sign and opposite-sign trileptonic final state.

Mass	SS: $(l^\pm l^\pm) l^\mp \nu$	OS: $(l^\pm l^\mp) l^\pm \nu$
40	4.220e+02	4.222e+02
50	2.980e+02	2.984e+02
60	1.690e+02	1.696e+02
70	5.920e+01	5.905e+01
80	5.350e+00	5.340e+00
90	2.010e+00	2.015e+00
100	1.020e+00	1.022e+00
125	3.150e-01	3.192e-01
150	1.390e-01	1.420e-01
175	7.180e-02	7.425e-02
200	4.130e-02	4.328e-02
250	1.670e-02	1.802e-02
300	7.960e-03	8.870e-03
350	4.200e-03	4.849e-03
400	2.370e-03	2.845e-03
500	8.760e-04	1.128e-03
600	3.700e-04	5.052e-04
700	1.720e-04	2.444e-04
800	8.670e-05	1.246e-04
900	4.640e-05	6.611e-05
1000	2.610e-05	3.618e-05
1250	7.440e-06	8.925e-06
1500	2.590e-06	2.508e-06

Since there are extra partonic processes included into the diagram in NLO cross section, the expectation is the NLO cross section to be higher than the LO cross section. Therefore, NLO cross section provides more realistic and reliable results while compared with the data [35-37]. However, we simulated LO cross section with LO and NLO PDFs due to the lack of NLO cross section processes in ALPGEN v2.14 generator. So, we expect to have more realistic and reliable outcomes by having LO cross section results with LO and NLO PDFs. The results in Table 3 and the comparison in the right plot of Figure 2 shows that the cross section results obtained with NLO PDF is slightly higher than the cross section results obtained with LO PDF. This is because extra partonic processes are included in the diagram in NLO.

4. Discussion and Conclusion

One of the extensions to the SM to explain the neutrino's mass origin is the Seesaw type-I model. In this model, light neutrinos ($\mu_\nu < 1$ eV) are produced with very heavy neutrinos at the TeV scale. In this study, the cross section predictions of heavy Majorana neutrino mass production via dileptonic and trileptonic channels at 8 and 13 TeV, center of mass energy in proton-proton collisions are provided.

For the cross section predictions, the HVYN package in the ALPGEN framework is used with LO CTEQ6L and CTEQ6L1, and NLO CTEQ6M PDFs. As expected, the cross section values at 13 TeV is higher than the 8 TeV results in all mass regions. The cross section results of heavy Majorana mass neutrinos for both same-sign and opposite-sign dilepton channels with a $p_T > 5$ GeV/c cut on leptons show a similar trend for the higher mass region starting from 300 GeV/c². The results show that if there is such heavy mass neutrino particles, producing them in dileptonic final state has a higher possibility than producing them in the trileptonic decay mode in proton-proton collisions.

We conclude that if the main interest is in making prediction on some new processes (such as heavy Majorana neutrinos) in some new kinematic region, not included in our global fit, then the difference in using LO PDF + LO matrix element and NLO PDF + LO matrix element is at higher order in α_s which is beyond the accuracy of the calculation we are performing. If the interest is in making prediction on some new process using, e.g., Madgraph with initial state parton showering, using a consistent showering code would be ideal. If the showering is done correctly only at the LO (such as the default in PYTHIA), then one should use LO PDF, though there are some recent efforts to incorporate a LO showering with NLO PDFs (and NLO matrix element).

Acknowledgment

This work was supported by Scientific Research Projects (BAP) of Erciyes University, Turkey under the grant contract of FDS-2021-10856.

References

- [1] S Chatrchyan, G Hmayakyan, V Khachatryan, A M Sirunyan, and W Adam et al. The CMS experiment at the CERN LHC. *Journal of Instrumentation*, 3(08):S08004–S08004, 2008. doi: 10.1088/1748-0221/3/08/s08004.
- [2] G Aad, E Abat, J Abdallah, A A Abdelalim, and A Abdesselam et al. The ATLAS experiment at the CERN large hadron collider. *Journal of Instrumentation*, 3(08):S08003–S08003, 2008. doi: 10.1088/1748-0221/3/08/s08003.
- [3] G. Aad, B. Abbott, J. Abdallah, S. Abdel Khalek, A. A. Abdelalim, and et. al. Search for supersymmetry in pp collisions at $\sqrt{s} = 7$ TeV in final states with missing transverse momentum and b-jets with the atlas detector. *Phys. Rev. D*, 85:112006, Jun 2012. doi: 10.1103/PhysRevD.85.112006.
- [4] Y. Fukuda, T. Hayakawa, E. Ichihara, K. Inoue, K. Ishihara, and et. al. Evidence for oscillation of atmospheric neutrinos. *Physics Review Letter*, 81:1562–1567, Aug 1998. doi: 10.1103/PhysRevLett.81.1562.
- [5] Q. R. Ahmad, R. C. Allen, T. C. Andersen, J. D. Anglin, G. Bühler, and et. al. Measurement of the rate of $\nu_e + d \rightarrow p + p + e^-$ interactions produced by ^8B solar neutrinos at the sudbury neutrino observatory. *Physics Review Letter*, 87:071301, Jul 2001. doi: 10.1103/PhysRevLett.87.071301.
- [6] Q. R. Ahmad, R. C. Allen, T. C. Andersen, J. D. Anglin, J. C. Barton, and al. et. Direct evidence for neutrino flavor transformation from neutral-current interactions in the sudbury neutrino observatory. *Phys. Rev. Lett.*, 89:011301, Jun 2002. doi: 10.1103/PhysRevLett.89.011301.
- [7] Peter Minkowski. $\mu \rightarrow e\gamma$ at a rate of one out of 10^9 muon decays? *Physics Letter B*, 67(4):421–428, 1977. doi: 10.1016/0370-2693(77)90435-X.

- [8] P. van Nieuwenhuizen and D.Z. Freedman. Supergravity: Proceedings of the Workshop, Stony Brook, N.Y., 27-29 September, 1979. North-Holland Publishing Company, 1979.
- [9] Akio Sugamoto Osamu Sawada. Proceedings of the Workshop on "The Unified Theory and the Baryon Number in the Universe. National Laboratory for High Energy Physics, 1979.
- [10] Rabindra N. Mohapatra and Goran Senjanović. Neutrino mass and spontaneous parity nonconservation. *Physics Review Letter*, 44:912–915, Apr 1980. doi: 10.1103/PhysRevLett.44.912.
- [11] M. Magg and Ch. Wetterich. Neutrino mass problem and gauge hierarchy. *Physics Letters B*, 94(1):61–64, 1980. doi: 10.1016/0370-2693(80)90825-4.
- [12] J. Schechter and J. W. F. Valle. Neutrino decay and spontaneous violation of lepton number. *Phys. Rev. D*, 25:774–783, Feb 1982. doi: 10.1103/PhysRevD.25.774.
- [13] Robert Foot, H. Lew, X. G. He, and Girish C. Joshi. See-saw neutrino masses induced by a triplet of leptons. *Zeitschrift für Physik C Particles and Fields*, 44:441–444, 1989. doi: 10.1007/BF01415558.
- [14] J. Schechter and J. W. F. Valle. Neutrino masses in $su(2)_c \times u(1)$ theories. *Physics Review D*, 22:2227–2235, Nov 1980. doi: 10.1103/PhysRevD.22.2227.
- [15] F. del Aguila and J.A. Aguilar-Saavedra. Distinguishing seesaw models at lhc with multi-lepton signals. *Nuclear Physics B*, 813(1):22–90, 2009
- [16] Wai-Yee Keung and Goran Senjanović. Majorana neutrinos and the production of the right-handed charged gauge boson. *Phys. Rev. Lett.*, 50:1427–1430, May 1983. doi:10.1103/PhysRevLett.50.1427.
- [17] Duane A. Dicus, Debra Dzialo Karatas, and Probir Roy. Lepton nonconservation at supercollider energies. *Phys. Rev. D*, 44:2033–2037, Oct 1991. doi: 10.1103/PhysRevD.44.2033.
- [18] A. Datta, M. Guchait, and A. Pilaftsis. Probing lepton number violation via majorana neutrinos at hadron supercolliders. *Phys. Rev. D*, 50:3195–3203, Sep 1994. doi: 10.1103/PhysRevD.50.3195.
- [19] F. M. L. Almeida, Y. A. Coutinho, J. A. Martins Simões, and M. A. B. do Vale. Signature for heavy majorana neutrinos in hadronic collisions. *Phys. Rev. D*, 62:075004, Sep 2000. doi: PhysRevD.62.075004.
- [20] O. Panella, M. Cannoni, C. Carimalo, and Y. N. Srivastava. Signals of heavy majorana neutrinos at hadron colliders. *Phys. Rev. D*, 65:035005, Jan 2002. doi: 10.1103/PhysRevD.65.035005.
- [21] Tao Han and Bin Zhang. Signatures for majorana neutrinos at hadron colliders. *Phys. Rev. Lett.*, 97:171804, Oct 2006. doi: 10.1103/PhysRevLett.97.171804.
- [22] Anupama Atre, Tao Han, Silvia Pascoli, and Bin Zhang. The search for heavy majorana neutrinos. *Journal of High Energy Physics*, 2009(05):030–030, may 2009. doi: 10.1088/1126-6708/2009/05/030.
- [23] O. Adriani, M. Aguilar-Benitez, S. Ahlen, J. Alcaraz, A. Aloisio, and et. al. Search for isosinglet neutral heavy leptons in z_0 decays. *Physics Letters B*, 295(3):371–382, 1992. doi: 10.1016/0370-2693(92)91579-X
- [24] P. Abreu, W. Adam, T. Adye, I. Azhinenko, G.D. Alekseev, and et. al. Search for neutral heavy leptons produced in Z decays. *Z. Phys. C*, 74:57–71, 1997. doi: 10.1007/s002880050370.
- [25] Georges Aad, Brad Abbott, Jalal Abdallah, Samah Abdel Khalek, and et. al. Search for heavy majorana neutrinos with the atlas detector in pp collisions at $\sqrt{s} = 8$ tev. search for heavy majorana neutrinos with the atlas detector in pp collisions at $\sqrt{s} = 8$ tev. *JHEP*, 07:162. 28 p, Jun 2015. doi: 10.1007/JHEP07(2015)162.
- [26] Morad Aaboud, Georges Aad, Brad Abbott, Ovsat Abidinov, Baptiste Abeloos, and et. al. Search for heavy Majorana or Dirac neutrinos and right-handed W gauge bosons in final states with two charged leptons and two jets at $\sqrt{s} = 13$ TeV with the ATLAS detector. Search for heavy Majorana or Dirac neutrinos and right-handed W gauge bosons in final states with two charged leptons and two jets at $\sqrt{s} = 13$ TeV with the ATLAS detector. *JHEP*, 1901:016. 51 p, Sep 2018. doi: 10.1007/JHEP01(2019)016.
- [27] S. Chatrchyan, V. Khachatryan, A.M. Sirunyan, A. Tumasyan, W. Adam, and et.al. Search for heavy majorana neutrinos in $\mu^\pm\mu^\pm$ +jets and $e^\pm e^\pm$ +jets events in pp collisions at s=7 tev. *Physics Letters B*, 717(1):109–128, 2012.
- [28] V. Khachatryan, A.M. Sirunyan, A. Tumasyan, W. Adam, T. Bergauer, and al. et. Search for heavy majorana neutrinos in $\mu^\pm\mu^\pm$ + jets events in proton-proton collisions at $\sqrt{s} = 8$ tev. *Physics Letters B*, 748:144–166, 2015. doi: 10.1016/j.physletb.2015.06.070.
- [29] Vardan Khachatryan, Albert M Sirunyan, Armen Tumasyan, Wolfgang Adam, Ece Asilar, and et. al. Search for heavy Majorana neutrinos in $e^\pm e^\pm$ + jets and $e^\pm\mu^\pm$ + jets events in proton-proton collisions at $\sqrt{s} = 8$ TeV. *Journal of High Energy Physics*, 04:169, 2016. doi: 10.1007/JHEP04(2016)169.

- [30] A. M. Sirunyan, A. Tumasyan, W. Adam, F. Ambrogi, E. Asilar, and et. al. Search for heavy majorana neutrinos in same-sign dilepton channels in proton-proton collisions at $\sqrt{s} = 13$ tev. *Journal of High Energy Physics*, 2019(1), 2019. doi: 10.1007/JHEP01(2019)122.
- [31] Michelangelo L. Mangano, Mauro Moretti Fulvio Piccinini, Antonio D. Polosa, and Roberto Pittau. Alpgen, a generator for hard multiparton processes in hadronic collisions. *Journal of High Energy Physics*, 2003(7):001, July 2003. doi: 10.1088/1126-6708/2003/07/001.
- [32] Lai, HL., Huston, J., Mrenna, S. et al. Parton distributions for event generators. *J. High Energ. Phys.* 2010, 35 (2010), doi: 10.1007/JHEP04(2010)035
- [33] Jonathan Pumplin et al., New Generation of Parton Distributions with Uncertainties from Global QCD Analysis, . *J. High Energ. Phys* (2002)012, doi: 10.1088/1126-6708/2002/07/012
- [34] Francisco del Aguila, Juan Antonio Aguilar-Saavedra, and Roberto Pittau. Heavy neutrino signals at large hadron colliders. *Journal of High Energy Physics*, 2007(10):047–047, 2007. doi: 10.1088/11266708/2007/10/047.
- [35] Kamuran Dilsiz, Emrah Tiras. Inclusive W boson QCD predictions and lepton charge asymmetry in proton-proton collisions at $\sqrt{s}= 14$ TeV, *Canadian Journal of Physics* 19 March 2018, doi: 10.1139/cjp-2017-0635
- [36] Hasan Ogul, Kamuran Dilsiz, Emrah Tiras, Ping Tan, Yasar Onel, and Jane Nachtman, High Order QCD Predictions for Inclusive Production of Bosons in Collisions at TeV, *Advances in High Energy Physics* , Volume 2016, Article ID 7865689 , doi: 10.1155/2016/7865689
- [37] Hasan Ogul, Kamuran Dilsiz,. Cross Section Prediction for Inclusive Production of Boson in pp Collisions at TeV: A Study of Systematic Uncertainty due to Scale Dependence, *Advances in High Energy Physics*, vol. 2017, Article ID 8262018, 8 pages, 2017. <https://doi.org/10.1155/2017/8262018>